ChemComm

COMMUNICATION

View Article Online
View Journal | View Issue

Cite this: *Chem. Commun.*, 2023, 59, 5289

Received 29th January 2023,
Accepted 6th April 2023

DOI: 10.1039/d3cc00406f

rsc.li/chemcomm

Partially fluorinated poly(arylene–alkane)s containing cobaltocenium for alkaline-stable anion exchange membranes†

Run Zhang,[ab] Xiaoyu Zhao,[ab] Wenhao Li,[abc] Huidong Qian *[ab] and Hui Yang *[ab]

Alkali-resistant metal-based cationic polyelectrolytes are designed as anion exchange membranes. After grafting aminocobaltocene hexafluorophosphates onto partially fluorinated ether-free poly(arylene–alkane)s *via* a simple nucleophilic substitution reaction, the membrane exhibits excellent chemical, thermal and mechanical stability, high hydroxide conductivity, as well as durability of single cells for 400 h.

Anion exchange membranes (AEMs) are one of the core devices of anion exchange membrane fuel cells (AEMFCs) and play an essential role in the performance and lifetime of AEMFCs.[1] AEMFCs have faster oxygen reduction reaction (ORR) kinetics and can use non-precious metal catalysts in alkaline environments, thus reducing costs compared to proton exchange membrane fuel cells (PEMFCs).[2] The commercialization of AEMs is still constrained by shortcomings such as inadequate performance and short lifetime.[3]

Applying AEMs requires high performance, long operational life, and excellent alkaline stability, which depends on the structure of the main chain, the type of cationic group, and the role of the main side chain.[4] The mechanical strength, thermal stability, and chemical stability of AEMs are determined by the main chain, which is developed from the initial industrial plastic material modification to the aryl ether bonded main chain and currently the aryl ether-free connected main chain.[5] For example, Miyatake *et al.* prepared partially fluorinated aromatic AEMs, which improve the mechanical strength and reduce the water absorption swelling of AEMs while providing specific alkaline stability.[6] Bae *et al.* first reported a series of high molecular weight poly(biphenyl alkylene)s with long side chains by superacid-catalyzed polymerization. These AEMs have excellent thermal, chemical, and mechanical stability.[7] Yang *et al.* blended poly(bis-arylimidazolium)s with polybenzimidazole, which provides a method to synthesize water-insoluble ether-free polymers with dicationic groups in the repeat unit.[8] Researchers have designed a series of poly(aryl piperidine)s without any weak benzyl hydrogen or aryl ether bonds, which have a stable backbone structure with relatively excellent chemical stability and mechanical strength, and also exhibit high electrical conductivity and perfect peak power density.[9] The superb performance makes this backbone one of the best choices for the next generation of AEMs.

In recent years, several cationic groups have been applied in AEMs, including quaternary ammonium (QA),[10] *N*-spirocyclic QA,[11] imidazolium,[8] guanidinium,[12] piperidinium,[13] quaternary phosphonium,[14] and metal complex cations.[15] Cationic groups attached to the polymer backbone in AEMs are susceptible to OH^- attack, which decreases the ionic conductivity, and alkaline stability due to the nucleophilic substitution (S_N2), Hofmann elimination (E2), or an ylide reaction in alkaline environments.[16]

Cobaltocenium has an excellent alkaline stability because of its unique, metal–ligand solid bond that limits the attack of OH^- on the central metal ion.[15d] Zhu *et al.* prepared AEMs containing cobaltocenium by introducing cobaltocenium into the polybenzimidazole backbone *via* a microwave polymerization, among which the hydroxide conductivity of MCp_2Co^+-PBI was 37.5 mS cm^{-1} at 90 °C. After 672 h of the alkaline stability test, the hydroxide conductivity only decreased by 15–20%, showing excellent alkaline stability.[15a] Yan *et al.* used the more alkaline-stable per-methyl cobaltocenium ($Cp^*_2Co^+$) to graft onto a polysulfone backbone, and the IEC loss of the $Cp^*_2Co^+$-PSf membrane was 18% and 27% of the initial value after immersion in 1 M KOH solution at 80 °C for 1000 h and 2000 h, respectively.[15d] Tang *et al.* utilized cobaltocenium derivatives as side chains of polyolefin backbones polymerized by ring-opening metathesis polymerization (ROMP). The conductivity was 90 mS cm^{-1} at 90 °C and remained above 95%

[a] *Shanghai Advanced Research Institute, Chinese Academy of Sciences, Shanghai 201210, China. E-mail: qianhd@sari.ac.cn, yangh@sari.ac.cn*
[b] *University of Chinese Academy of Sciences, Beijing 100049, China*
[c] *School of Physical Science and Technology, ShanghaiTech University, Shanghai 201210, China*

† Electronic supplementary information (ESI) available: Detailed preparation and characterization of monomers, AEMs and MEAs. Fuel cell test procedures. See DOI: https://doi.org/10.1039/d3cc00406f

after immersion in 1 M NaOH solution for more than a month, indicating an excellent alkaline stability.[17]

Herein, we report the facile preparation of a partially fluorinated poly(arylene–alkane) containing cobaltocenium,[18] by introducing fluorinated aromatic rings in the backbone to facilitate the formation of microphase separations and the construction of intra-membrane hydrophilic–hydrophobic channels, thereby increasing the OH^- conduction rate. As shown in Scheme 1 and Fig. S1–S8 (ESI†), partially fluorinated poly(arylene–alkane) (PFTP) with a weight-average molecular weight of 208 kDa and a polydispersion index of 3.3 (Fig. S9, ESI†) was firstly prepared by the superacid-catalyzed polymerization, then a one-step reaction was also carried out to prepare aminocobaltocene hexafluorophosphates (H_2N-Cp_2Co^+) by the simple and efficient direct amination of cobaltocene.[19] A series of high-performance, low-swelling rate metal-based AEMs containing cobaltocenium were successfully prepared by grafting H_2N-Cp_2Co^+ onto fluorinated aromatic backbones *via* a simple nucleophilic substitution reaction, and the content of cobaltocenium was easily controlled by adjusting the feed ratios of PFTP and H_2N-Cp_2Co^+ monomers.

Due to the insolubility of PFTP-Cp_2Co_x, the chemical structure was firstly confirmed by Fourier transform infrared (FT-IR) spectroscopy. Comparing the FT-IR spectra before and after grafting (Fig. S10, ESI†), it can be seen that the PFTP-$Cp_2Co_{0.8}$ membrane has a new C–N bond stretching vibration absorption peak at 1277 cm^{-1}, and a deformation vibration peak of the N–H bond at 1603 cm^{-1}, confirming the successful introduction of cobaltocenium groups into the PFTP polymer matrix.

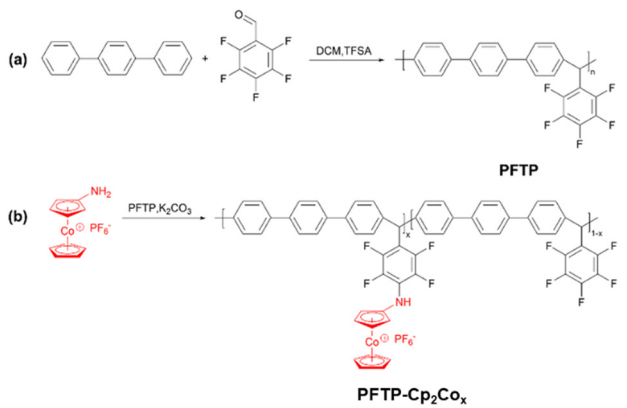

Scheme 1 Synthetic routes of (a) PFTP polymer and (b) PFTP-Cp_2Co_x membranes.

Fig. S11 (ESI†) shows the comparison of the cobaltocenium and the membranes before and after grafting by UV-visible spectroscopy (UV-vis). The two characteristic peaks at 305 and 405 nm are attributed to the π–π* and n–π* transitions of H_2N-Cp_2Co^+, respectively. The peaks of the PFTP-$Cp_2Co_{0.8}$ membrane after grafting are observed at 306 and 405 nm, thus proving that the cobaltocenium has been successfully introduced into the polymer. The cobalt elemental valence analysis of the PFTP-$Cp_2Co_{0.8}$ membrane by X-ray photoelectron spectroscopy (XPS) (Fig. S12, ESI†) corresponds to the peaks of $Co_2P_{3/2}$ and $Co_2P_{2/2}$ of Co^{3+} at 784 eV and 799 eV, respectively, confirming that the cobalt in cobaltocenium is present in the polymer in the Co^{3+} valence state. The above characterization demonstrated that the cobalt dichloride cation was successfully grafted onto the PFTP membrane substrate in the Co^{3+} form.

Water absorption is one of the critical factors in the ionic conductivity and dimensional stability of AEMs. High water absorption will cause severe membrane distortion and poor dimensional stability, while low water absorption will result in low ionic conductivity of the membrane.[20] The introduction of pentafluorobenzaldehyde monomers is essential for preparing high molecular weight polymers, reducing water absorption, and enhancing ionic conductivity.[21] The actual ion exchange capacity (IEC) of PFTP-Cp_2Co_x membranes was calculated by back-titration; the water uptake (WU) rate and the adsorptive swelling rate (SR) of the membranes were determined at 20 °C and 80 °C (Table 1). As the grafting degree increases, the WU of the membrane increases from 4.5% at the beginning to 7.0% at 20 °C, and the SR also rises slightly from 1.6% to 2.3%, which shows that the membranes have good dimensional stability. The lower SR showed good swelling resistance of the membranes. The highest hydroxide conductivity of 75.8 mS cm^{-1} is achieved at 80 °C with the PFTP-$Cp_2Co_{0.8}$ membrane. In contrast, the low WU, low IEC, and high conductivity indicate high utilization of the adsorbed water, which is attributed to the hydrophobic structure of the pentafluorobenzaldehyde and the hydrophilic network of the cationic groups constructing highly hydrophilic-hydrophobic channels within the membranes, facilitating the rapid transport of hydroxide. The unstained PFTP-$Cp_2Co_{0.8}$ membrane has a distinct pro-hydrophobic microphase separation structure in the transmission electron microscopy (TEM) image (Fig. S13, ESI†).

The ionic conductivity plays a vital role in AEMFCs, as shown in Fig. 1a, where the hydroxide conductivity increases with temperature. The hydroxide conductivity of the PFTP-$Cp_2Co_{1.0}$ membrane with the highest grafting degree is as high

Table 1 Ion exchange capacity (IEC), water uptake (WU), and swelling rate (SR) of PFTP-Cp_2Co_x membranes

			WU (%)		SR (%)		Conductivity (mS cm^{-1})	
Polymer	IEC[a] (mmol g^{-1})	IEC[b] (mmol g^{-1})	20 °C	80 °C	20 °C	80 °C	20 °C	80 °C
PFTP- $Cp_2Co_{0.6}$	1.16	1. 07	4.5	5.2	1.6	1.9	23.3	61.9
PFTP- $Cp_2Co_{0.8}$	1.44	1.36	5.8	6.3	2.1	2.3	28.3	75.8
PFTP-$Cp_2Co_{1.0}$	1.68	1.52	7.0	7.9	2.3	2.5	32.6	89.3

[a] Theoretical IEC. [b] Experimental IEC.

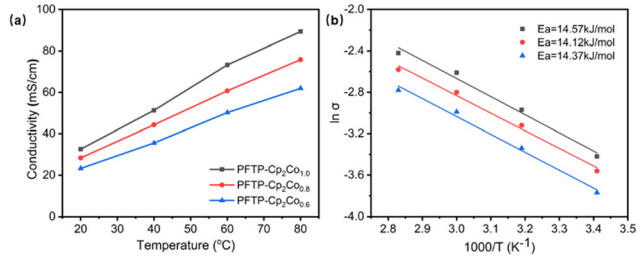

Fig. 1 (a) OH^- conductivity of PFTP-Cp_2Co_x membranes at varied temperatures. (b) Arrhenius plots of hydroxide conductivity for the PFTP-Cp_2Co_x membranes.

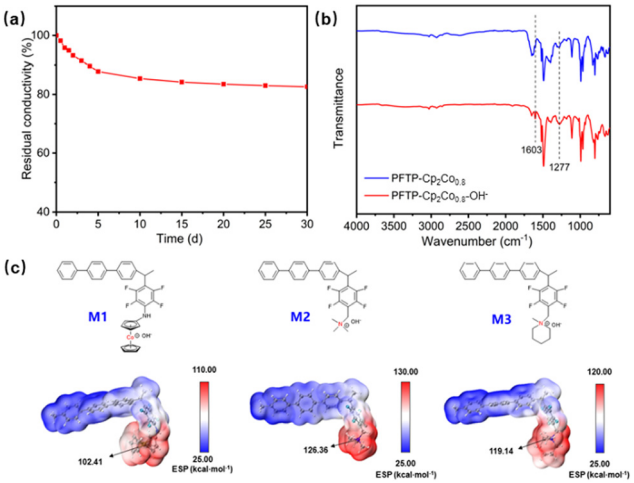

Fig. 2 (a) OH^- conductivity variation of the PFTP-$Cp_2Co_{0.8}$ membrane in 1 M KOH at 80 °C for 30 days. (b) FT-IR spectra of the PFTP-$Cp_2Co_{0.8}$ membrane before and after alkaline treatment (PFTP-$Cp_2Co_{0.8}$: without alkali treatment; PFTP-$Cp_2Co_{0.8}$-OH^-: treated in 1 M KOH at 80 °C for 30 days). (c) ESP of cobaltocenium M1, quaternary ammonium M2, and piperidinium M3.

as 89.3 mS cm^{-1} at 80 °C, which is consistent with the IEC variation pattern. The variation of the hydroxide conductivity of AEMs with temperature is consistent with Arrhenius behavior, and the activation energy (E_a) of the hydroxide transport mechanism was calculated by fitting the curve. As shown in Fig. 1b, the E_a calculated from the straight-line slope is in the range of 14.12–14.57 kJ mol^{-1}, which indicates that this series of membranes have a good hydroxide conductivity efficiency and require low energy to overcome the barrier. In addition, the apparent E_a of the PFTP-Cp_2Co_x membranes is comparable to or slightly lower than those of the other reported AEMs (10–23 kJ mol^{-1}),[22] suggesting that these membranes have a water-promoted hydroxide transport mechanism similar to other hydrated AEMs.

As shown in Fig. S14 (ESI†), the membranes' weight loss with temperature is recorded by observing thermogravimetric analysis (TGA). The PFTP membrane has an excellent thermal stability at 500 °C before the degradation of the backbone structure. The cobaltocenium group undergoes decomposition between 250 °C and 480 °C. The degradation temperature drops slightly as the degree of grafting increases, but all of them are much higher than the FC operating temperature. The mechanical properties of the grafted PFTP-$Cp_2Co_{0.8}$ membrane were determined by measuring the stress–strain curves of the polymeric precursors and AEM samples using an electro-mechanical universal testing machine (EUTM) (Fig. S15, ESI†), which is essential for the long-term operation of the AEM. The tensile strength of the PFTP membrane is 21.7 MPa, whereas that of the PFTP-$Cp_2Co_{0.8}$ membrane is 24.2 MPa. The stress of the PFTP-$Cp_2Co_{0.8}$ membrane is enhanced, possibly due to the introduction of hydrophilic groups that increase water absorption. Meanwhile, the elongation at break of the PFTP-$Cp_2Co_{0.8}$ membrane is 1.9% compared to 3.2% for the PFTP membrane, which is a decrease due to the greater rigidity of the cobaltocenium side groups. Hence, the PFTP-$Cp_2Co_{0.8}$ membrane possesses excellent mechanical stability for practical application.

The alkaline stability of the cationic group is one of the essential factors in determining the working life of AEMFCs. The PFTP-$Cp_2Co_{0.8}$ membrane shows no rupture or significant changes when immersed in a 1 M KOH solution at 80 °C for 30 days. The conductivity decreases relatively quickly during the initial 5 days, followed by a gradual conductivity reduction, with excellent alkaline stability of 82.6% conductivity retention after 30 days (Fig. 2a). To further verify the alkaline stability of the PFTP-$Cp_2Co_{0.8}$ membrane, the chemical structure of a 30 days alkali-treated membrane was compared with those of pristine membranes by FT-IR. In the FT-IR spectra of the PFTP-$Cp_2Co_{0.8}$ membrane before and after immersion in 1 M KOH at 80 °C (Fig. 2b), there is no significant degradation of the structure, which corresponds to the retention of conductivity, thus demonstrating the excellent alkaline stability of the PFTP-$Cp_2Co_{0.8}$ membrane.

Three model compounds with similar structures were further designed to understand the alkaline stability of the as-prepared membranes. The corresponding electrostatic potential (ESP) was calculated *via* density flooding theory. As shown in Fig. 2c, the three compounds are the cobaltocenium (M1), the quaternary ammonium (QA) (M2), and the piperidinium (M3), and the molecules have been labeled with their ESP surface maxima, which are calculated based on the optimized structures. The structures of the studied molecules are fully optimized at the B3LYP-D3BJ/def2-SVP level of view. The electrostatic attraction to the hydroxide ion thus makes it more susceptible to hydroxide ion attack, leading to the degradation of the cationic group. Cations with higher ESP are known to be more sensitive to attack by the hydroxide anion due to the stronger electrostatic attraction between the cation and the hydroxide anion. M1 has a theoretically calculated ESP of 102.41 kcal mol^{-1}, which has more vital base stability than M2 at 126.36 kcal mol^{-1} and M3 at 119.14 kcal mol^{-1} (Fig. 2c). Therefore, cobaltocenium has better alkaline stability than piperidinium and QA.

As the PFTP-$Cp_2Co_{1.0}$ membrane is more rigid and prone to rupture, the PFTP-$Cp_2Co_{0.8}$ membrane is selected for FC performance testing due to its suitable electrical conductivity and mechanical stability. As the current density increases, the polarization effect of the electrode leads to a reduction in cell

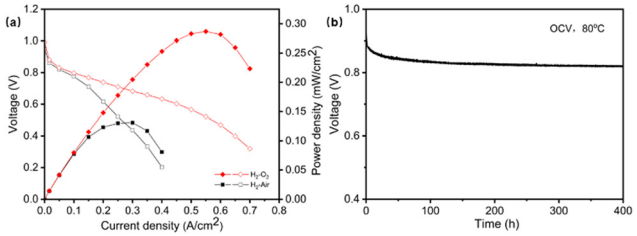

Fig. 3 (a) Polarization curves and power density curves of MEA under H_2/air, H_2/O_2 conditions, respectively. Test conditions: 80 °C with H_2 (400 sccm) and air (400 sccm) or O_2 (400 sccm) at 100% RH and 1 bar backpressure. Pt–Ru and Pt loadings for the anode and cathode were 0.41 mg cm^{-2} and 0.34 mg cm^{-2}, respectively. (b) OCV test of PFTP-$Cp_2Co_{0.8}$-based MEA supplying H_2 and air for 400 h. Test conditions: 80 °C with H_2 (400 sccm) and air (400 sccm) at 100% RH without backpressure.

voltage. The membrane electrode assembly (MEA) has an effective surface area of 2.5 × 2.5 cm^2. The AEMFC performance of the MEA was tested under H_2/air and H_2/O_2 conditions. As shown in Fig. 3a, the open circuit voltage (OCV) of FC for H_2/air and H_2/O_2 conditions at 80 °C is 0.949 V and 0.991 V, respectively.

These indicate that the membrane can inhibit gas permeation relatively well. A peak power density of 131 mW cm^{-2} is achieved at a current density of 300 mA cm^{-2} under H_2/air conditions. The FC reaches a peak power density of 287 mW cm^{-2} at a current density of 550 mA cm^{-2} under H_2/O_2 conditions. The PFTP-$Cp_2Co_{0.8}$ membrane has superior single cell performance compared to the other metal-based AEMs but is inferior to the most non-metal-based membranes (Tables S1 and S2, ESI†). Durability tests were carried out by recording the OCV at 80 °C and 100% relative humidity. Fig. 3b shows that no rapid degradation of OCV is observed throughout the trial. After 400 h, the OCV slowly decreases from 0.949 V to 0.820 V with a reduction of 0.32 mV h^{-1}. Gradual OCV decay can be caused by complex factors such as ionomers, AEMs, catalyst degradation, side chain breakage, and MEA manufacturing techniques. The power density of the AEMFC can be further optimized by improving the MEA preparation process.

In summary, cobaltocenium containing AEMs were prepared by the superacid-catalyzed polymerization of a partially fluorinated aromatic backbone followed by a facile nucleophilic substitution reaction. The rigid ether-free backbone of PFTP and alkaline stability of the cobaltocenium groups provide excellent swelling resistance and appropriate mechanical properties to the AEMs. The introduction of hydrophobic fluorine-containing groups and hydrophilic cationic groups constructs hydrophobic channels, further improving the ionic conductivity. The AEMFC using cobaltocenium containing polyelectrolyte delivers a peak power density of 287 mW cm^{-2} under H_2/O_2 conditions and excellent MEA stability for 400 h, demonstrating the potential promise for the preparation of AEMs.

Financial support from the National Key Research and Development Program of China (2018YFB1502301) and the National Natural Science Foundation of China (22279157) is gratefully acknowledged.

Conflicts of interest

There are no conflicts to declare.

Notes and references

1 D. W. Shin, M. D. Guiver and Y. M. Lee, *Chem. Rev.*, 2017, **117**, 4759–4805.
2 M. M. Hossen, M. S. Hasan, M. R. I. Sardar, J. B. Haider, Mottakin, K. Tammeveski and P. Atanassov, *Appl. Catal., B*, 2023, **325**, 121733.
3 J. Zhang, W. Zhu, T. Huang, C. Zheng, Y. Pei, G. Shen, Z. Nie, D. Xiao, Y. Yin and M. D. Guiver, *Adv. Sci.*, 2021, **8**, 2100284.
4 (*a*) Z. Tao, C. Wang, X. Zhao, J. Li and M. D. Guiver, *Adv. Mater. Technol.*, 2021, **6**, 2001220; (*b*) Z. Y. Zhu, W. W. Gou, J. H. Chen, Q. G. Zhang, A. M. Zhu and Q. L. Liu, *J. Membr. Sci.*, 2021, **636**, 119569; (*c*) K. Yang, X. Chu, X. Zhang, X. Li, J. Zheng, S. Li, N. Li, T. A. Sherazi and S. Zhang, *J. Membr. Sci.*, 2020, **603**, 118025.
5 X. Li, K. Yang, Z. Li, J. Guo, J. Zheng, S. Li, S. Zhang and T. A. Sherazi, *Int. J. Hydrogen Energy*, 2022, **47**, 15044–15055.
6 A. M. Ahmed Mahmoud and K. Miyatake, *J. Mater. Chem. A*, 2018, **6**, 14400–14409.
7 (*a*) W. H. Lee, Y. S. Kim and C. Bae, *ACS Macro Lett.*, 2015, **4**, 814–818; (*b*) W. H. Lee, E. J. Park, J. Han, D. W. Shin, Y. S. Kim and C. Bae, *ACS Macro Lett.*, 2017, **6**, 566–570.
8 N. Yu, J. Dong, T. Wang, Y. Jin, W. Tang and J. Yang, *Polymer*, 2022, **240**, 124491.
9 (*a*) J. S. Olsson, T. H. Pham and P. Jannasch, *Adv. Funct. Mater.*, 2018, **28**, 1702758; (*b*) H. Peng, Q. Li, M. Hu, L. Xiao, J. Lu and L. Zhuang, *J. Power Sources*, 2018, **390**, 165–167; (*c*) J. Wang, Y. Zhao, B. P. Setzler, S. Rojas-Carbonell, C. Ben Yehuda, A. Amel, M. Page, L. Wang, K. Hu, L. Shi, S. Gottesfeld, B. Xu and Y. Yan, *Nat. Energy*, 2019, **4**, 392–398.
10 X. Li, K. Yang, Z. Li, J. Guo, J. Zheng, S. Li, S. Zhang and T. A. Sherazi, *Int. J. Hydrogen Energy*, 2022, **47**, 15044–15055.
11 T. H. Pham, J. S. Olsson and P. Jannasch, *J. Mater. Chem. A*, 2018, **6**, 16537–16547.
12 Q. Wang, L. Huang, J. Zheng, Q. Zhang, G. Qin, S. Li and S. Zhang, *J. Membr. Sci.*, 2022, **643**, 120008.
13 (*a*) J. Li, C. Yang, S. Wang, Z. Xia and G. Sun, *RSC Adv.*, 2022, **12**, 26542–26549; (*b*) D. Pan, P. M. Bakvand, T. H. Pham and P. Jannasch, *J. Mater. Chem. A*, 2022, **10**, 16478–16489.
14 B. Zhang, H. Long, R. B. Kaspar, J. Wang, S. Gu, Z. Zhuang, B. Pivovar and Y. Yan, *RSC Adv.*, 2018, **8**, 26640–26645.
15 For examples of cationic metallo-polyelectrolytes, see: (*a*) N. Chen, H. Zhu, Y. Chu, R. Li, Y. Liu and F. Wang, *Polym. Chem.*, 2017, **8**, 1381–1392; (*b*) T. Zhu, Y. Sha, H. A. Firouzjaie, X. Peng, Y. Cha, D. Dissanayake, M. D. Smith, A. K. Vannucci, W. E. Mustain and C. Tang, *J. Am. Chem. Soc.*, 2020, **142**, 1083–1089; (*c*) X. Liu, N. Xie, J. Xue, M. Li, C. Zheng, J. Zhang, Y. Qin, Y. Yin, D. R. Dekel and M. D. Guiver, *Nat. Energy*, 2022, **7**, 329–339; (*d*) S. Gu, J. Wang, R. B. Kaspar, Q. Fang, B. Zhang, E. Bryan Coughlin and Y. Yan, *Sci. Rep.*, 2015, **5**, 11668.
16 N. Chen and Y. M. Lee, *Prog. Polym. Sci.*, 2021, **113**, 101345.
17 T. Zhu, S. Xu, A. Rahman, E. Dogdibegovic, P. Yang, P. Pageni, M. P. Kabir, X. D. Zhou and C. Tang, *Angew. Chem. Int. Ed.*, 2018, **57**, 2388–2392.
18 V. M. Velasco, M. G. Zolotukhin, M. T. Guzmán-Gutiérrez, S. L. Morales and S. Fomine, *Macromolecules*, 2008, **41**, 8504–8512.
19 M. Jochriem, D. Bosch, H. Kopacka and B. Bildstein, *Organometallics*, 2019, **38**, 2278–2279.
20 F. Wang, D. Wang and Y. Nagao, *ChemSusChem*, 2021, **14**, 2694–2697.
21 S. Gottesfeld, D. R. Dekel, M. Page, C. Bae, Y. Yan, P. Zelenay and Y. S. Kim, *J. Power Sources*, 2018, **375**, 170–184.
22 B. Sana, A. Das and T. Jana, *ACS Appl. Energy Mater.*, 2022, **5**, 3626–3637.

